

## DYNAMICAL STRUCTURE OF ONE-PHASE MODEL OF SOLID COMBUSTION

MICHAEL FRANKEL

Department of Mathematical Sciences,  
Indiana University–Purdue University Indianapolis,  
Indianapolis, IN 46202-3216

AND

VICTOR ROYTBURD

Department of Mathematical Sciences  
Rensselaer Polytechnic Institute,  
P.O. Box 2604  
Troy, NY 12180-3590

**Abstract.** We present results of numerical study of complex dynamics generated by the one-phase free-boundary problem with kinetics modeling gasless combustion. We study dynamical structure generated by the problem using bifurcational diagrams obtained through correlational dimension. In the case of periodically varying initial concentration the problem exhibits frequency locking. We also demonstrate that a finite-dimensional reduction via the method of collocations leads to a similar dynamical structure

**1. Introduction.** The paper continues a discussion on the dynamics due to Stefan type [3] problems with kinetics, in particular the phenomenon of frequency locking as a response to a periodic perturbation of the initial concentration. We give a brief description of the rigorous results concerning well-posedness, and discuss numerical simulation of the one-phase problem and its finite-dimensional imitation that is derived via collocation method.

The one-sided free-boundary problem (FBP) represents a mathematical model of condensed-state combustion (also known as combustion synthesis cf. [13]), assuming that the heat conduction in the product state is much slower than in the fresh combustible mixture. Similar model is obtained for instance for the laser induced evaporation from the surface of metals [1]. The numerical simulation described in [2] demonstrated that the unperturbed FBP generates a variety of complex thermokinetic oscillations including Hopf bifurcation, period doubling cascades, Shilnikov-Hopf bifurcation etc.

After the occurrence of these dynamical features of FBP have been established, it would be interesting to understand how the orbits of different complexity correspond to the (usually more than one) physical parameters. Below we present

---

*Key words and phrases.* Key words: free boundary, Stefan problem, correlation dimension, bifurcation diagram, mode locking .

M. Frankel's work is partially supported by NSF under Grant DMS-0207308.

bifurcation diagrams in the parameter space based on the correlation dimension for both: the constant and the variable concentration of the combustible..

Indeed, the new feature that was added in [3] is a periodic perturbation of the initial concentration of the so-called deficient component which directly effects the velocity of the free boundary. As a result we observe a variety of quasi-periodic and complex periodic regimes with periods that are various multiples of the perturbation period. This is a clear manifestation of the classical phenomenon of frequency locking.

The physical phenomena modeled by periodically driven dynamical systems appear in many fields (see e.g. [14]) such as lasers, superconductors (Josephson's junctions), mechanical engineering, etc. These systems are known to exhibit complex patterns of behavior including entrainment. The bands of locked modes typically have the appearance of the so called Arnol'd tongues in the amplitude-frequency parameter space.

It is necessary to mention that the analysis of externally periodically (in time) forced systems is usually carried out for an appropriate physically motivated ansatz leading to a low-dimensional ODE. In our case we are not aware of any physical considerations on which such reduction can be based. However, in the last section we carry out truncation to a finite-dimensional system using the collocation method and compare its dynamical structure with that of the original FBP using the bifurcation (dynamics) diagrams.

The diagrams for both: FBP and the finite-dimensional system in the amplitude-frequency space show typical Arnol'd tongues. One should realize that in the case of FBP every point in the parameter space is a result of DNS of a computationally nontrivial problem. Luckily it turns out that even a rough approximation of the correlation dimension is sufficient to distinguish between the periodic and aperiodic orbits. To the best of our knowledge this method has not been previously used for bifurcation diagrams of such type.

**2. The one-sided free-boundary problem.** Combustion of condensed matter represents a self-sustained wave of exothermic chemical reaction that transforms a solid combustible mixture directly into a solid product. The appropriately non-dimensionalized 1-D one-phase model consists of heat diffusion in the combustible mixture

$$u_t = u_{xx}, \quad x < s(t), \quad u(x, 0) = u_0(x) \geq 0, \quad (1)$$

supplemented by the kinetics condition

$$v(t) = Z_0(s(t)) g[u(s(t), t)], \quad (2)$$

and the Stefan-type condition at the free boundary moving in the negative direction:

$$u_x(s(t), t) = -v(t), \quad (3)$$

where  $v(t)$  is the boundary velocity,  $s(t) = \int_0^t v(\tau) d\tau$  is its position,  $u$  is the temperature. At  $-\infty$  the the temperature of the fresh combustible is assumed to be zero  $u(-\infty, t) = 0$ .

Under reasonable assumptions on the kinetics functions  $g$ , one can prove that problem (1)-(3) possesses global in time, uniformly bounded classical solutions (cf. [6] for the  $Z \equiv 1$  case).

**Theorem 1.** *Let  $0 < Z_{\min} \leq Z_0(x) \leq Z_{\max}$  be a Lipschitz continuous function. Suppose that the kinetic functions  $g$  satisfies the following assumptions:  $g(u)$  is*

a continuous, monotone decreasing, negative function with bounded derivative on  $(0, \infty)$  and  $g(0) = -g_0$  for some  $g_0 > 0$ ; and  $\lim_{u \rightarrow \infty} g(u)/u = 0$ . Then for continuous and bounded initial data there exists one and only one classical solution of the free interface problem (1)-(3). The solution is uniformly bounded for all  $t > 0$ .

Note that  $v_0 = g_0 Z_{\min}$  is the minimal possible speed of the boundary. The central point of the global existence proof is the *a priori* estimate:

**Theorem 2.** Let  $u(x, t), v(t)$  be a classical solution of the free interface problem (1)-(3) and  $\sup_{-\infty < x < \infty} |u_0(x)| = M$ , then  $|u(x, t)| \leq 2(g_1/v_0 + M)/Z_{\min}$  where  $g_1$  is a constant dependent on the kinetic function  $g$ .

Since  $v = Z_0[s(t)]g[u(s(t), t)]$ , for the velocity we have the obvious bound  $|v| \leq Z_{\max}g(2(M + g_1/v_0)/Z_{\min})$

In addition one can show that FBP (1)-(3) is dissipative and possesses a global compact attractor of a finite Hausdorff dimension [6, 7]. It is important to emphasize that the rigorous results lead to a deeper understanding of the dynamics generated by the FBP, and provide an additional degree of confidence in the numerical simulations.

**3. Dynamics of unperturbed problem.** Before we discuss the phase locking for a nonhomogeneous concentration  $Z_0(x)$  several remarks are due regarding the basic problem with  $Z_0(x) \equiv 1$ . It is convenient to represent the kinetics in the form:

$$g(u) := 1 + \alpha J(u) \quad (4)$$

where the function  $J(\xi) = (g(\xi) - 1)/\alpha$  is normalized so that  $J(1) = 0$ ,  $J'(1) = -1$ . This makes the problems with different kinetics identical in terms of linearization about the basic solution. while  $\alpha > 0$  is the main instability parameter of the problem. The variables are selected so that the *boundary propagates to the left*.

Problem (1)-(3) has a unique traveling wave solution

$$u_b = \exp(x + t), \quad x \leq -t, \quad s_b = -t. \quad (5)$$

provided  $J$  is monotone. A linear stability analysis indicates that the loss of stability occurs via a supercritical Hopf bifurcation at  $\alpha_{cr} = 3$ , at the frequency  $\omega_{cr} = \sqrt{3}$ . For appropriate ranges of parameters the system exhibits a Feigenbaum cascade and transition to chaos, a Shilnikov-Hopf bifurcation etc. (see [2] for details).

It is necessary to mention that the exact functional form of the kinetics for solid combustion is not known. In DNS we used Arrhenius type kinetics

$$g_{\alpha, \sigma}(u) = -\exp[\alpha(u - 1)/(1 + \sigma(u - 1))]; \quad (6)$$

"transplanted" from the gas combustion, and a power kinetics (defined through its inverse)

$$g_{\alpha, q}^{-1}(v) = 1 + \frac{1}{\alpha} [(-v)^q - (-v)^{-p}] / (p + q) \quad (7)$$

where  $p, q > 0$  are additional parameters allowing to control subtle changes of its shape. We put  $p = 1$  in the DNS discussed below. Both kinetics satisfy conditions required for the rigorous results formulated above. It turns out that many complex dynamical features are also observed for both. In order to better understand the response of FBP to the kinetics parameters we need to see how different dynamical regimes are situated in the parameter space.

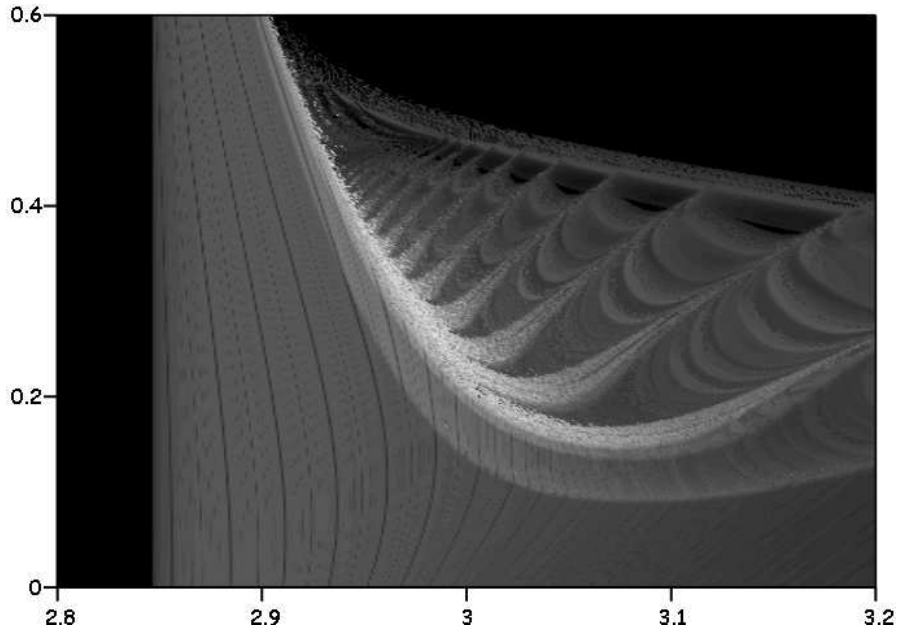


FIGURE 1. Bifurcation diagram for FBP with Arrhenius kinetics (1) in  $\alpha\sigma$ -plane. Resolution  $400 \times 400$ .

**4. Bifurcation structure via correlation dimension.** To demonstrate possible dynamic scenarios in the parameter space we employ asymptotic (for  $t$  large) correlation dimension of the orbits (see [5] for the discussion of correlation dimension in the context of unperturbed free-interface problems). To the best of our knowledge, this is the first application of correlation dimension for the investigation of the bifurcation structure, in particular for PDEs.

We are primarily interested in the qualitative understanding of dynamics, in particular in the distinction between periodic and aperiodic regimes. Our experience shows that the bifurcation structure computed via correlation dimension is largely insensitive to the sample (finite-dimensional projection of the phase space) size  $\geq 2$ . Only thanks to this circumstance are we able to obtain a detailed bifurcation map at a reasonable computational cost.

For DNS we employed a finite-difference scheme in the coordinate system attached to the interface  $\eta = x - s(t)$  (see [?] for detail). In mathematical terms FBP in (1)-(3) generates the temporal evolution in the infinitely-dimensional “phase” space of functions  $u(\eta, \cdot)$  and scalars  $v$ .

Every point on the dynamics diagrams is therefore a result of DNS of a nontrivial FBP, and the computational cost of a detailed map becomes prohibitive. To make the problem with  $1.6 \times 10^5$  DNS tractable from the computational viewpoint, we have to choose a rather crude space mesh size. Consequently the critical values for the bifurcation parameter  $\alpha$  undergo some shift from the theoretical values: for example, the value  $\alpha = 5.2$  corresponds to a simple periodic relaxational oscillation for the unperturbed problem.

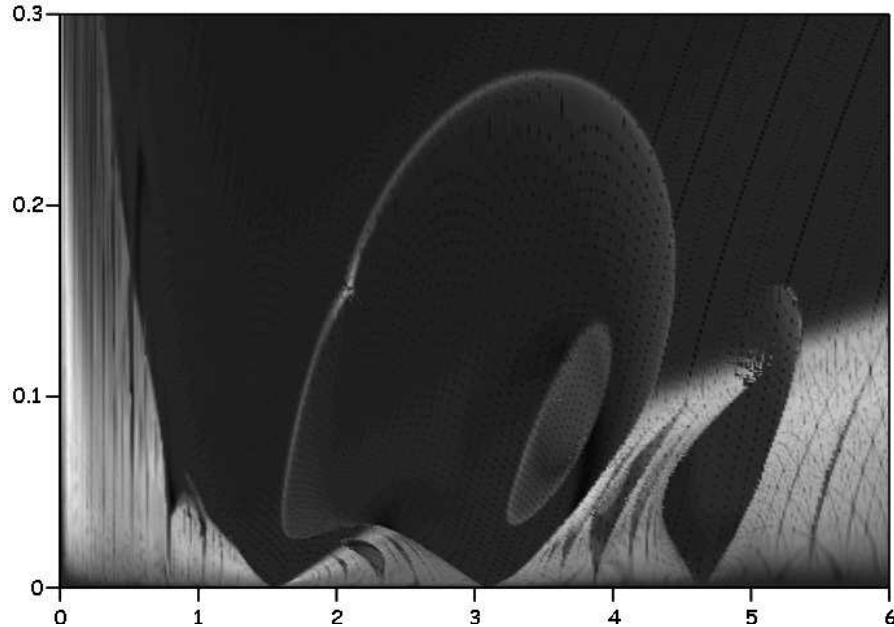


FIGURE 2. Bifurcation diagram for periodically perturbed FBP (1)-(3) with power kinetics in the  $\omega a$ -plane. Resolution  $400 \times 400$ .

Fig.(1) depicts dynamical structure of the "unperturbed" ( $Z_0(x) \equiv 1$ ) FBP (1)-(3) with the kinetics (6) in the  $\alpha\sigma$ -plane. The kinetics parameters  $\alpha$  and  $\sigma$  vary in the intervals  $[2.8, 3.2]$  and  $[0, .6]$  respectively with 400 mesh points in each variable.

The darker areas, corresponding to lower correlation dimension represent periodic orbits, while the lighter areas correspond to aperiodic orbits. The darkest vertical strip on the left corresponds to the subcritical in the sense of Hopf bifurcation stable basic solutions. Remarkably, in spite of the crudeness of truncation the results show that the method is sensitive enough to even differentiate somewhat between periodic orbits of different period (multiplicity). For instance, one can clearly distinguish the transition to period doubling when  $\alpha$  increases as a slightly lighter shade. The lightest feather-like structure inside corresponds to the chaotic solutions.

**5. Dynamics generated by FBP with periodic initial concentration.** Next we discuss DNS of the forced FBP (1)-(3), with the initial mass concentration

$$Z_0(x) = 1 + a \cos(\omega x) \quad (8)$$

Note that the initial concentration in (1)-(3) is a function of the dependent variable of the problem  $s(t)$ . Consequently, the driving frequency  $\omega$  and the temporal frequency of the periodic solutions, as in Fig.(3) are not the same.

Fig.(2) represents a bifurcation diagram for (1)-(3) with kinetics (7) in the frequency-amplitude ( $\omega a$ ) plane. One can clearly recognize classical Arnol'd tongs structure. We observe increasingly narrower secondary tongs corresponding to periodic orbits of higher multiplicity. Remarkably, correlation dimension is able to capture even rather fine transitions between qualitatively different periodic regimes. Although theoretically the correlation dimension of any periodic regime is equal to

1, in the vicinity of the bifurcation convergence to the attractor is very slow. This is reflected in the higher values of the *numerical* approximation for the dimension. For example, the large lightly shaded oval contour separates between simple periodic (above the oval) and double-periodic (inside) orbits.

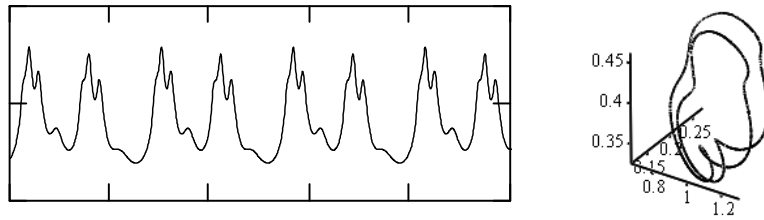


FIGURE 3. Subharmonic periodic solution of FBP  $a = .1$ ,  $\omega = 5$   
Boundary temperature  $u(0, t)$  vs. time  $400 \leq t \leq 450$

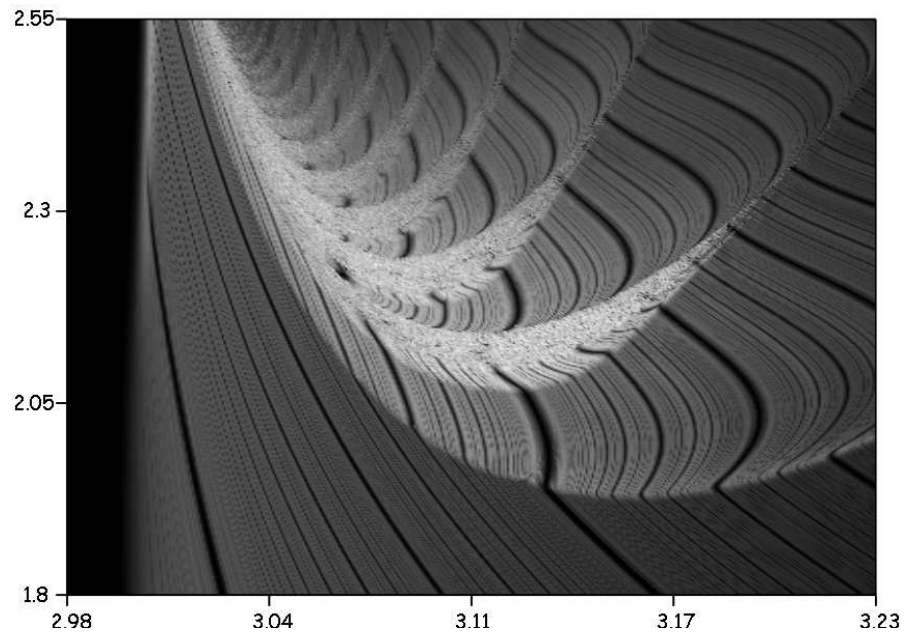
There are a number of complex features observed in dynamical response of some known finite-dimensional counterparts of our FBP such as, for instance, the forced van der Pol equation [11, 12] that one would attempt to verify. For instance, whether the Arnol'd tongues represent a dense set with its complement forming a Cantor set in the  $(a, \omega)$ -plane, whether the Feigenbaum sequences occur within the tongues etc. It would also be interesting to investigate how the frequency locking response changes with increasing  $\alpha$ .

Fig.(3) depicts a typical frequency locking periodic orbit. in the subharmonic region (note that the forcing has a *spatial* not temporal period) represented by the time history of the boundary temperature  $u(\eta, t)|_{\eta=0}$ . The display on the right is a 3-d projection of the orbit that lives in an infinitely-dimensional phase space. As parameters of forcing vary, one encounters a wide range of complex periodic, quasi-periodic and chaotic orbits. We remark that quasi-periodic solutions with more than two basic periods have also been observed.

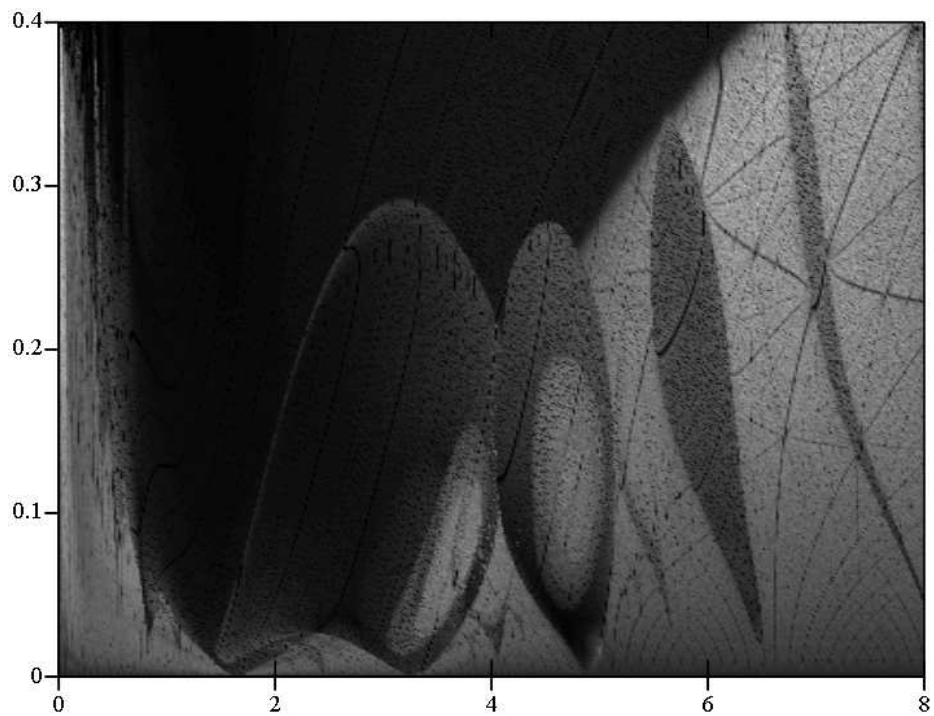
**6. Finite-dimensional model.** A qualitative approximation by a 3-d dynamical system was derived in [9, 8] (for  $Z \equiv 1$ ) using the collocation method as follows. First in the coordinate attached to the free boundary  $z = x - s(t)$  the problem becomes

$$\begin{aligned} u_t - vu_z - u_{zz} &= 0, z < 0, \\ u_z(0, t) &= -v(t), \quad v(t) = -Z_0(s(t)) g[u(0, t)] \end{aligned} \quad (9)$$

We select  $n$  collocation points  $z_1 = 0 > z_2 > \dots > z_n$ . and seek an approximation for the solution in the form  $u(z, t) = \sum_{k=1}^{n+1} a_k(t) \phi_k(z)$ . A convenient basis in our case consists of  $\phi_i(z) = z^i e^z$ . We demand that Eq. (9) is satisfied exactly at the collocation points, as well as the boundary conditions at  $z = 0$ . We set  $n = 3$ , and select  $z_1 = 0, z_2 = -1, z_3 = -2$ . As a result we obtain the following system of



Bifurcation diagram for the unperturbed finite-dimensional system (10) with power kinetics in the  $\alpha q$ -plane. Resolution  $400 \times 400$ .



Bifurcation diagram for the periodically perturbed finite-dimensional system (10) with power kinetics in the  $\omega a$ -plane. Resolution  $400 \times 400$ .

ordinary differential equations:

$$\begin{aligned}\dot{d}_1 &= -3d_1 - 2d_2 + d_3 + 9w + w(4w - d_2 + d_1 + d_3) \\ \dot{d}_2 &= -6d_1 - 6d_2 + 3d_3 + 24w + w(9w - 2d_2 + 3d_1 + 3d_3) \\ \dot{d}_3 &= d_2 - d_3 - w(3 + w) \\ \dot{s} &= w - 1\end{aligned}\tag{10}$$

supplemented by  $w = -g(1 + d_3)Z_0(s)$ , where  $w = v + 1$ ,  $d_2 = 2a_2 + 3w + 3$ ;  $d_1 = 2a_1 + w + 1$ ,  $d_3 = a_4 - 1$  are new variables for which the equations are automatically resolved with respect to the derivatives; and, in addition, the equilibrium of the unperturbed case ( $Z \equiv 1$ ) is now at 0. It is easy to find that there is a Hopf bifurcation at  $\alpha_{cr} = 3$  with  $\omega_{cr} = \sqrt{3}$ . Note that  $\alpha_{cr}$  and  $\omega_{cr}$  are exactly the same as for the FBP.

For the unperturbed case  $Z_0(s) \equiv 1$  the  $3 \times 3$  system (10) was shown to be dynamically similar to the FBP [8]. Thus, it is interesting to compare its bifurcation diagram Fig. (5) with that of FBP Fig. (1). One cannot help noticing a fair measure of similarity between the two at least in the general outline, although Fig. (1) was obtained for a different kinetics. The areas corresponding to chaotic behavior are feather-like bent structures. The two diagrams differ in finer details, in particular (5) has a system of dark stripes that seems to have a Cantor set structure. We hope to comment on the dynamical interpretation of such curious dynamical features in the near future.

Next we compare the bifurcation diagram Fig (6) for the periodically perturbed by (8) system (10) to that of FBP Fig (2). First it clearly indicates that the finite-dimensional system exhibits entrainment as well. Once again there is a degree of similarity between the FBP and the finite-dimensional model, perhaps more so when the forcing frequency is closer to the natural frequencies of the respective Hopf bifurcations  $\omega_{cr}$ . Farther away the similarity fades and we observe for instance two Arnold's tongues merge and separate again as  $a$  increases. Subtler details of the diagrams can be revealed by a "computational zoom in". A more detailed study of the diagrams with dynamical interpretations of the transitions between different areas may lead in our view to interesting new observations regarding the dynamics of the system. Finally we present an example of a periodic solution of the forced

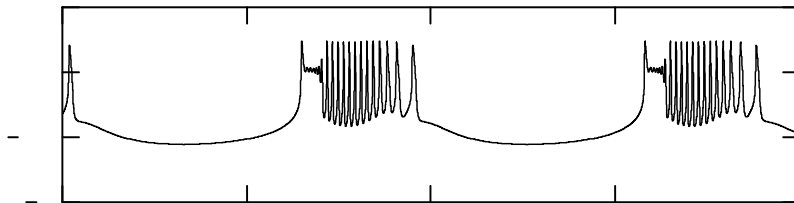


FIGURE 4. Subharmonic periodic bursts generated by the finite-dimensional system  $a = 0.3$ ,  $\omega = 0.05$

by (8) finite-dimensional model (10). Fig. (4) shows the time evolution of the free-boundary temperature for a subharmonic perturbation. One can easily observe that

the frequency is locked by a bursting type dynamics which seems to be typical in the deeply subharmonic region of frequencies.

*Acknowledgements.* M Frankel's work was partially supported under the NSF Grant DMS- 0207308

#### REFERENCES

- [1] S. M. Gol'berg and M. I. Tribelskii, On laser induced evaporation of nonlinear absorbing media, *Zh. Tekh. Fiz. (Sov. Phys.-J. Tech. Phys.)* **55**, 848-857 (1985).
- [2] M. Frankel and V. Roytburd, Dynamical portrait of a model of thermal instability: cascades, chaos, reversed cascades and infinite period bifurcations, *Int. J. of Bifurcation and Chaos*, **4** (1994), 579-593.
- [3] M. Frankel and V. Roytburd, Frequency locking for a combustion synthesis front propagating through a periodic medium, *Phys. Let. A*, Vol **329**/1-2 (2004) pp 68-75
- [4] M. Frankel and V. Roytburd, Exothermic interface propagation in periodic media, in preparation.
- [5] M. Frankel and V. Roytburd, Low fractal dimension of attractors for a one-phase nonequilibrium Stefan problem, *DCDS*, Suppl. Vol., (2003), 281-287
- [6] M. Frankel and V. Roytburd, Compact attractors for a free-boundary model of exothermic phase transitions , *EJDE* **15** (2002), 1-27
- [7] M. Frankel and V. Roytburd, Finite Dimensional Attractor for a One-Phase Stefan Problem with Kinetics, *J. Dynamics Diff. Eqs.* **15**(2003) No.1, 87-106
- [8] M. Frankel, G. Kovacic, V. Roytburd and I. Timofeyev, Finite-dimensional dynamical system modeling thermal instabilities, *Physica D* **137** (2000), 295-315
- [9] M. Frankel and V. Roytburd, Finite-dimensional model of thermal instabilities, *Appl. Math. Let.*, **8** (1995), 39-44
- [10] P. M. Krishenik, A. G. Merzhanov, and K. G. Shkadinskii, Nonstationary Regimes of Transformation of Multilayered Heterogeneous Systems, *Combustion, Explosion, and Shock Waves*, Vol. **38**, No. 3, (2002) pp. 313-321.
- [11] M. Levi, Qualitative analysis of the periodically forced relaxation oscillations, *Memoirs Amer. Math. Soc.* **32** 244 (1981), 1-147.
- [12] R. Mettin, U. Parlitz and W. Lauterborn, Bifurcation structure of the driven van der Pol oscillator, *International J Bifurcation Chaos* **3** (1993) 1529-1555.
- [13] A. Varma, A. S. Rogachev, A. S. Mukasyan and S. Hwang, Combustion synthesis of advanced materials, *Adv. Chem. Eng.* **24** (1998), 79-226.
- [14] F. Verhulst, Parametric and autoparametric resonance, *Acta Applicande Mathematicae* **70** (2002), 231-264.

*E-mail address:* mfrankel@math.iupui.edu